CERN-EP/82-122
6 August 1982

EUROPEAN ORGANISATION FOR NUCLEAR RESEARCH

# TRANSVERSE ENERGY DISTRIBUTIONS IN THE CENTRAL CALORIMETERS

UA1 Collaboration, CERN, Geneva, Switzerland

G. Arnison[10], A. Astbury[10], B. Aubert[2], C. Bacci[9], R. Bernabei[9], A. Bézaguet[4], R. Böck[4], T.J.V. Bowcock[6], M. Calvetti[4], T. Carroll[4], P. Catz[2], S. Centro[4], F. Ceradini[9], J. Ciboroski[11], S. Cittolin[4], A.M. Cnops[4], C. Cochet[11], J. Colas[2], M. Corden[3], D. Dallman[12], S. D'Angelo[9], M. DeBeer[11], M. Della Negra[2], M. Demoulin[4], D. Denegri[11], D. DiBitonto[4], L. Dobrzynski[7], J.D. Dowell[3], M. Edwards[3], K. Eggert[1], E. Eisenhandler[6], N. Ellis[3], P. Erhard[1], H. Faissner[1], G. Fontaine[7], J.P. Fournier[11], R. Frey[8], R. Frühwirth[12], G. Garvey[3], S. Geer[7], C. Ghesquière[7], P. Ghez[4], K.L. Giboni[1], W.R. Gibson[6], Y. Giraud-Heraud[7], A. Givernaud[11], A. Gonidec[2], G. Grayer[10], P. Gutierrez[8], R. Haidan[4], T. Hansl-Kozanecka[1], W.J. Haynes[10], L.O. Hertzberger[*], C. Hodges[8], D. Hoffmann[1], H. Hoffmann[4], D.J. Holthuizen[*], R.J. Homer[3], A. Honma[6], W. Jank[4], P.I.P. Kalmus[6], V. Karimäki[5], R. Keeler[6], I. Kenyon[3], A. Kernan[8], R. Kinnunen[5], H. Kowalski[4], W. Kozanecki[8], D. Kryn[7], F. Lacava[4], J.P. Laugier[11], J.P. Lees[2], H. Lehmann[1], R. Leuchs[1], A. Leveque[11], D. Linglin[2], E. Locci[11], M. Loret[11], J.J. Malosse[11], T. Markiewicz[4], G. Maurin[4], T. McMahon[3], J.P. Mendiburu[7], M.N. Minard[2], M. Moricca[9], H. Muirhead[4], F. Muller[4], A.K. Nandi[10], L. Naumann[4], A. Norton[4], A. Orkin-Lecourtois[7], L. Paoluzi[9], G. Piano Mortari[4], M. Pimïa[5], A. Placci[4], E. Radermacher[1], J. Ransdell[8], H. Reithler[1], J. Rich[11], M. Rijssenbeek[4], C. Roberts[10], C. Rubbia[4], B. Sadoulet[4], G. Sajot[7], G. Salvi[6], G. Salvini[9], J. Sass[11], J. Saudraix[11], A. Savoy-Navarro[11], D. Schinzel[4], W. Scott[10], T.P. Shah[10], M. Spiro[11], J. Strauss[12], K. Sumorok[3], F. Szoncso[12], C. Tao[4], J. Timmer[4], G. Thompson[6], E. Tscheslog[1], J. Tuominiemi[5], J.P. Vialle[4], J. Vrana[7], V. Vuillemin[4], H. Wahl[12], P. Watkins[3], J. Wilson[3], M. Yvert[2], E. Zurfluh[4]

Aachen[1]-Annecy (LAPP)[2]-Birmingham[3]-CERN[4]-Helsinki[5]-Queen Mary College, London[6]-Paris (Coll.de France)[7]-Riverside[8]-Roma[9]-Rutherford Appleton Lab.[10]-Saclay (CEN)[11]-Vienna[12] Collaboration

Presented to the XXI International Conference on High Energy Physics
Paris 26-31 July 1982

* NICKHEF, Amsterdam, The Netherlands

Abstract

We have measured the transverse energy distributions as seen by the central UA1 calorimeters up to ∿ 100 GeV. We demonstrate that the transverse energy measured in the calorimeters is strongly correlated with the charged multiplicity measured in the central detector.

The UA1 detector [1] is based on a dipole magnet which produces a transverse magnetic field of 0.7 T over a volume 7 x 3.5 x 3.5 $m^3$. In the middle of the magnet, surrounding the interaction region, is the central detector, a 6 m long x 2.2 m diameter drift chamber with image readout. The central calorimetry [$5^0 < \theta < 175^0$] surrounding this chamber has been used in conjunction with the central detector to study the characteristics of minimum bias events at $\sqrt{s}$ = 540 GeV.

The central calorimeters are shown in fig. 1 and their physical properties are summarised in Table I. The barrel electromagnetic calorimeter is made up from 24 semicylindrical counters on each side of the beams. These counters are lead (1.2 mm) and scintillator (1.5 mm) sandwiches approximately 4 m long in arc ($\Delta\phi \simeq \pi$) and 22 cm wide in the beam direction. They are $\simeq$ 26 radiation lengths thick, and are read out in four segments in depth. Each of the end cap electromagnetic calorimeters ($5^0 < \theta < 25^0$) comprises 32 radial sectors, of lead (4 mm) and scintillator (6 mm) sandwiches, 27 radiation lengths thick, arranged in 4 depth segments. This detector measures transverse energy $E_T$ directly since the read out is at $\theta \simeq 25^0$, and the attenuation length of the scintillator has been chosen to match the variation of $\sin\theta$ between $5^0$ and $25^0$. A position detector, consisting of proportional tubes permits the reconstruction of the energy off-line.

The hadron calorimeter has 5 cm thick iron plates with 1 cm scintillator throughout. The barrel region is covered by the eight C-shaped sections on each side ; these make up the return yoke of the magnet. They have 16 x 5 cm of iron, which is read out in two equal samplings in depth. Each end of the experiment is covered by 6 vertical I-shaped columns of laminated iron (23 x 5 cm). The granularity of this calorimeter depends on the distance from the beam as shown in Figure 1. It is read out in two equal depth sampling, and the coil of the magnet (20 cm aluminium) effectively acts as the first plate.

All of the UA1 calorimeters have been studied extensively in test beams in order to measure their resolution and response, and to determine the absolute energy scale. In the case of the electromagnetic calorimeters this energy calibration has been transferred to the collider experiment by means of a 4 Curie $Co^{60}$ source. This $Co^{60}$ source has also been used in situ to map and monitor the spatial response of the electromagnetic calorimeters as a function of time. The absolute energy scale for the hadron calorimeter has been obtained using cosmic-ray muons and the measured response to hadrons relative to muons of the test modules. β-sources, which could be placed in reproducible positions on some of the scintillators, were used to check the calibration. The photomultipliers on all calorimeters had their gains monitored by means of laser calibration systems using fibre optics.

Despite the high centre of mass energy at the collider (540 GeV), the UA1 central calorimeters measure mostly energy deposited by particles of < 1 GeV for the minimum bias data discussed in this paper. At these low energies hadrons deposit a significant fraction of their energy in the electromagnetic calorimeter. It is therefore most important to know well the hadronic response of the electromagnetic calorimeters. This response function has been measured in test beams [2] and also been confirmed using data from the present experiment by comparing measured momenta of isolated tracks with the energies recorded in the struck calorimeter cell. In the global features of events described here we have used an average response correction for the energy measured in the electromagnetic calorimeters. This, together with the non-linear response of the hadron calorimeters at low energies, introduces a scale uncertainty in summed transverse energy ($E_T$) of $\sim$ 15%. Using a simple Monte Carlo to simulate the effects of the resolution smearing and the energy dependence of the response correction we can conclude that the measured $E_T$ in the calorimeters is indeed the same as the overall incident transverse energy that one started with.

Data were taken with a minimum bias interaction trigger defined by a ± 20 ns coincidence in signals from hodoscopes placed ± 6.2 m on the proton and anti-proton arms. In addition data were also taken with the added requirement that the summed transverse energy in the central calorimeters be above some threshold (typically $E_T$>30 or 40 GeV). The magnetic field was mostly switched on but a sizeable part of the data was recorded with the field off. The results described in the following sections are based exclusively on the field off minimum-bias data. The distributions have been normalized to an inelastic cross-section of 40 mb

In order to ensure a pure beam-beam interaction several cuts were made. Tight timing coincidence cuts, together with a requirement that the reconstructed vertex be within ± 20 cm of its mean position along the beam direction, removed ∿ 30% of the triggered data leaving a sample of ∿ 20000 events used in this analysis. The summed transverse energy, $E_T$, was calculated using the relationship $E_T=\sum E_i \sin\theta_i$ where $E_i$ is the energy seen in the i-th calorimeter cell subtending a polar angle of $\theta_i$ with respect to the collision axis.

Figure 2 shows the $E_T$ spectrum for the full acceptance of the central calorimeters ($-3<\eta<3$ and $\Delta\phi=2\pi$) together with the $E_T$ distributions for various sub-regions in pseudorapidity and the azimuth. The curve represents a QCD parton-level prediction for the $E_T$ distribution at $\sqrt{s}$ = 540 GeV due to Fox and Kelly [3], which accounts for the contribution of gluon-bremstrahlung but does not include the effects of hadronization. It is clear that, within the framework of this QCD model, one would need to go to considerably higher transverse energies before these jets give an appreciable contribution. Figs. 2b to 2d show the effect of reducing the $\Delta\eta$, $\Delta\phi$ acceptance. It can be seen that the resulting distributions become more exponential with decreasing acceptance. The mean values and slopes of the exponential parts of the distributions are observed to scale approximately with the $\Delta\eta$, $\Delta\phi$ acceptance; such a feature is reminiscent of the behaviour of multiplicity. Fig. 2d shows a comparison of the $E_T$ distributions obtained by us and that of NA5 [4] for similar acceptance. The difference between the two can largely be attributed to the higher multiplicity attained at the collider energy.

In order to explore the relationship between the total transverse energy and the multiplicity we show in fig. 3 the $E_T$ distribution in the central region ($-3 \leq \eta \leq 3$) in terms of a KNO type variable [5] defined as $z = E_T/\langle E_T \rangle$ and compare this with the measured multiplicity distribution [6] (in the KNO variable $z = n/\langle n\rangle$) shown as the solid curve. It can be seen that the two shapes are strikingly similar. The observed differences in the tail region can be accounted for by a Monte Carlo model (discussed more fully below) which takes into account details of the $p_t$ spectrum and the smearing introduced by the response factor, particle masses etc. The model prediction is shown as the dashed curve in fig.3.

Fig. 4a shows the variation of mean transverse energy with the observed number of charged particles. A roughly linear increase of the $\langle E_T \rangle$

with charged multiplicity is observed. Fig. 4b shows the detailed behaviour of $< E_T>$ per observed charged particle with the observed multiplicity. After an initial decrease, this ratio shows a small linear increase with the observed multiplicity. The latter increase mirrors perfectly the measured increase in $< p_t>$ with charged multiplicity using momentum reconstructed tracks in the central detector [7]. The dashed line in Fig. 4b shows the Monte Carlo model prediction for this ratio. The increase in $< E_T>$/observed track at low multiplicities is also indicated by the Monte Carlo and is due to the higher number of neutrals at low multiplicities.

The simple Monte Carlo model used to calculate the curves displayed in figs. 3 and 4 had the following ingredients :

(i) Tracks were generated uniformly in rapidity with dN/dy = 3.3

(ii) Total/charged multiplicity was chosen randomly to give a mean of 1.7

(iii) The particle mixture was chosen in the ratio 3.6 $\pi^{\pm}$, 1.8 $\pi^{0}$, .3 $K^{\pm}$, .3 $K^{0}$ and .6 $\eta^{0}$.

(iv) The experimentally measured $p_t$ and multiplicity distributions were used.

(v) Fluctuation in energy deposited by charged tracks were taken as measured in our data and test beams.

It should be emphasised that a neutral/charged ratio significantly larger than 1:2 is required in order to account for the observed $<E_T>$/charged particle.

## Conclusions

(a) The $E_T$ distributions show that the shapes and mean values are the same for equal $\Delta\eta$, $\Delta\phi$ acceptance, becoming increasingly exponential as the acceptance is reduced.

(b) The scaled $E_T$ distribution (in $z = E_T/< E_T>$) shows a striking similarity to the scaled multiplicity distribution plotted in the KNO variable ($z = n/<n>$).

(c) We demonstrate that the $E_T$ measured in the calorimeter is strongly correlated with the charged multiplicity measured in the central detector. The < $E_T$> per charged particle increases with charged multiplicity for $n_{ch} \geq 20$, mirroring the observed increase in < $p_t$> with charged multiplicity measured using the central detector with field-on data. The < $E_T$> per particle is consistent with that measured using the central detector providing that a sufficient neutral/charged ratio is allowed for.

Acknowledgements

We should like to thank the members of the CERN Accelerator Divisions for their work in commissioning the SPS Collider and providing the collisions which have yielded this physics. We are extremely grateful to the CERN management and staff who have supported the UA1 experiment so generously, and extend these warm thanks to the following external sources of financial support :

Fonds zur Forderung der Wissenschaftlichen Forshung, Austria.
Valtion luonnontieteellinen toimikunta, Finland.
Institut National de Physique Nucléaire et de Physique des Particules and Institut de Recherche Fundamentale (CEA), France.
Bundesministerium fur Forschung und Technologie, Germany.
Istituto Nazionale di Fisica Nucleare, Italy.
Science and Engineering Research Council, United Kingdom.
Department of Energy, USA

A great deal of understanding was demanded of all these bodies in order that we could realise the UA1 detector on the timescale required. Our technical and engineering colleagues in the collaborating institutes provided the untiring support needed to build UA1 ; without their efforts we would have nothing to report, and we deeply acknowledge their work. Thanks are also due to the following people who have worked with the collaboration in the preparation and data collection on the runs described here, D. Cline, G. Petrucci, P. Queru, M. Steuer, H. Verweij and R. Wilson.

References

1a) Aachen-Annecy (LAPP)-Birmingham-CERN-London (Queen Mary College)-Paris (Collège de France)-Riverside-Roma-Rutherford-Saclay (CEN)-Vienna Collaboration, "A 4π solid-angle detector for the SPS used as a proton-antiproton collider at a centre-of-mass energy of 540 GeV. Proposal CERN/SPSC/78-06/P92 (1978).

b) M. Barranco Luque et al., Nucl. Instr. and Methods 176 (1980) 175.

c) M. Calvetti et al., Nucl. Instr. and Methods 176 (1980) 255.

d) K. Eggert et al., Nucl. Instr. and Methods 176 (1980) 217 and 223.

e) A. Astbury, Phys. Scripta 23 (1981) 397.

f) M. Calvetti, "The UA1 central detector", Talk given at the Int. Conf on Instrumentation for Colliding Beam Physics, SLAC, Stanford Feb. 1982.

g) S. Cittolin, "The UA1 data acquisition system", Talk given at the Int. Conf. on Instrumentation for Colliding Beam Physics, SLAC, Stanford, 17-23 Feb. 1982

h) "First results from the UA1 detector at the SPS Collider", UA1 Collaboration. Presented by B. Sadoulet at the XVIIth Rencontre de Moriond, 20-26 March 1982.

i) "The CERN proton-antiproton collider program". Presented by P.I.P. Kalmus at the International Workshop on Very High Energy Interactions in Cosmic Rays. University of Pennsylvania, April 1982.

2) M.J. Corden et al., Phys. Scripta 25 (1982) 5
M.J. Corden et al., Phys. Scripta 25 (1982) 11

3) G.C. Fox and R.L. Kelly, Caltech Preprint, CALT-68-890 (LBL-13985).

4) "A study of Deep Inelastic..." Bari-Krakov-Liverpool-München (MPI)-Nijmegen Collaboration, MPI-PAE/Exp.El.101.

5) Z. Koba, H.B. Nielson and P. Oleson, Nucl. Phys. B40 (1972) 317.

6) "Charged Particle Multiplicity Distributions...." UA1 Collaboration, Contribution to the Intern.Conf. on High Energy Physics, Paris, July 1982.

7) "Transverse momentum spectra for charged particles at the CERN proton-antiproton collider", UA1 Collaboration, Contribution to the Intern. Conf. on High Energy Physics, Paris, July 1982.

TABLE I

| Calorimeter | Sampling step | Thickness<br>$X_0$=Radiation L.<br>X=Absorption L. | Depth segments<br>in readout | Solid angle<br>Coverage | Cell Size | Resolution |
|---|---|---|---|---|---|---|
| EM<br>Barrel | 1.2 mm lead<br>1.5 mm scintillator | 26 $X_0$ | 3.3:6.6:9.9:6.6 $X_0$ | $25^\circ \le \theta \le 155^\circ$<br>$\phi \sim 2\pi$ | $\Delta\theta \sim 5^\circ$<br>$\Delta\phi \sim 2\pi$ | $0.15/\sqrt{E}$ |
| EM<br>End-Cap | 4.0 mm lead<br>6.0 mm scintillator | 27 $X_0$ | 4:7:9:7 $X_0$ | $5^\circ \le \theta \le 25^\circ$<br>$\phi \sim 2\pi$ | $\Delta\theta \sim 20^\circ$<br>$\Delta\phi \sim 11^\circ$ | $0.12/\sqrt{E}$ |
| Hadron<br>Barrel | 5 m iron<br>1 cm scintillator | 4.9 X | 2.5:2.5 X | $25^\circ \le \theta \le 155^\circ$<br>$\phi \sim 2\pi$ | | $0.8/\sqrt{E}$ |
| Hadron<br>End-Cap | 5 m iron<br>1 cm scintillator | 7.1 X | 3.5:3.5 X | $5^\circ \le \theta \le 25^\circ$<br>$\phi \sim 2\pi$ | | $0.8/\sqrt{E}$ |

Figure Captions

1. The UA1 central calorimeters.

2. $d\sigma/dE_T$ spectra for various acceptances as shown on the figures.

3. $E_T$ distribution for $|\eta| \leq 3$ in the KNO type variable $z = E_T / \langle E_T \rangle$. The solid and dashed curves are discussed in the text.

4a) Average $E_T$ vs observed charged multiplicity.
 b) Average $E_T$ per observed charged particle vs the observed multiplicity. The dashed curve is discussed in the text.

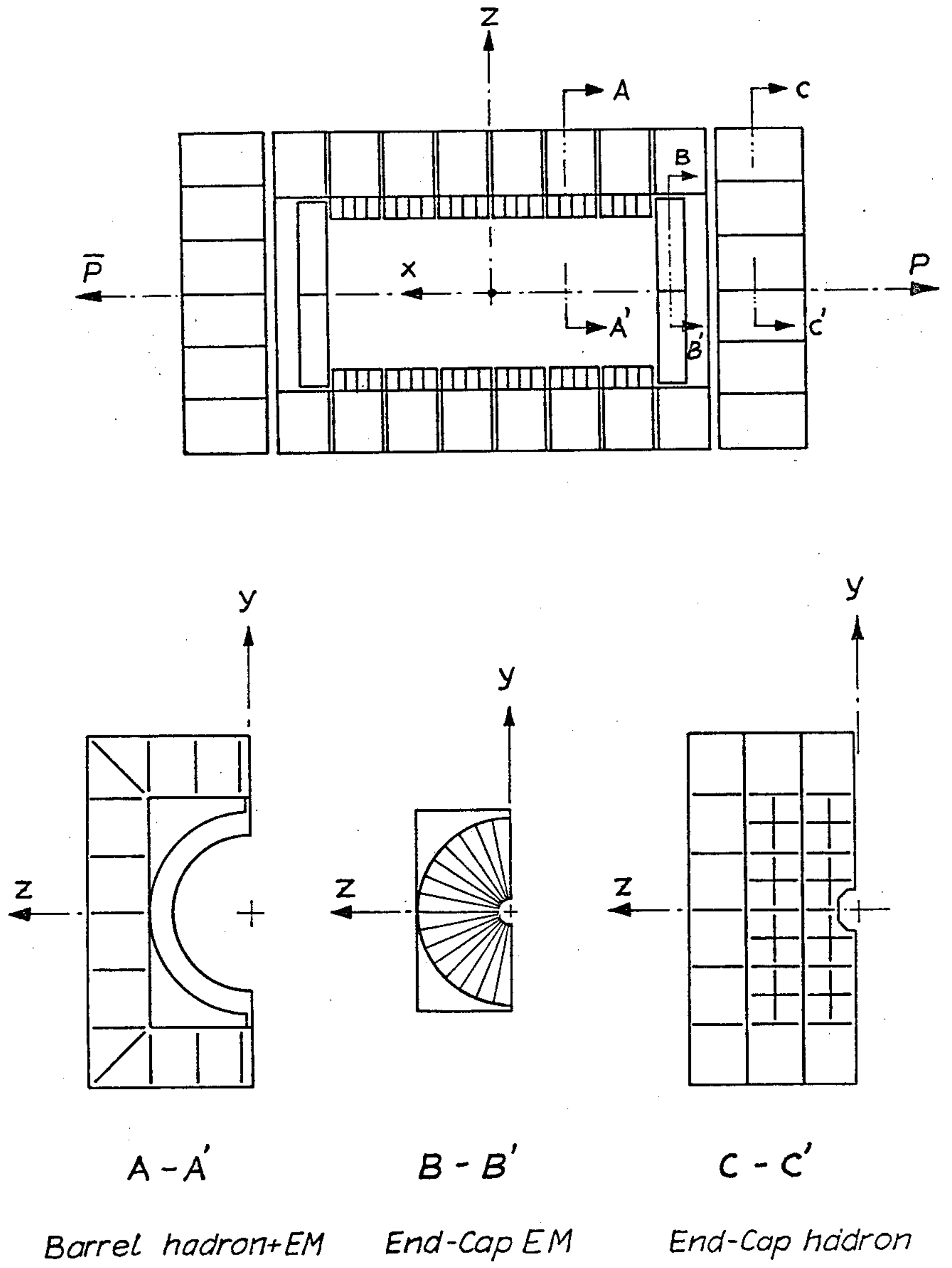
z
A
C
B
P̄
x
P
A'
B'
C'
y
z
A - A'
B - B'
C - C'
Barrel hadron+EM
End-Cap EM
End-Cap hadron
1m

Fig.1

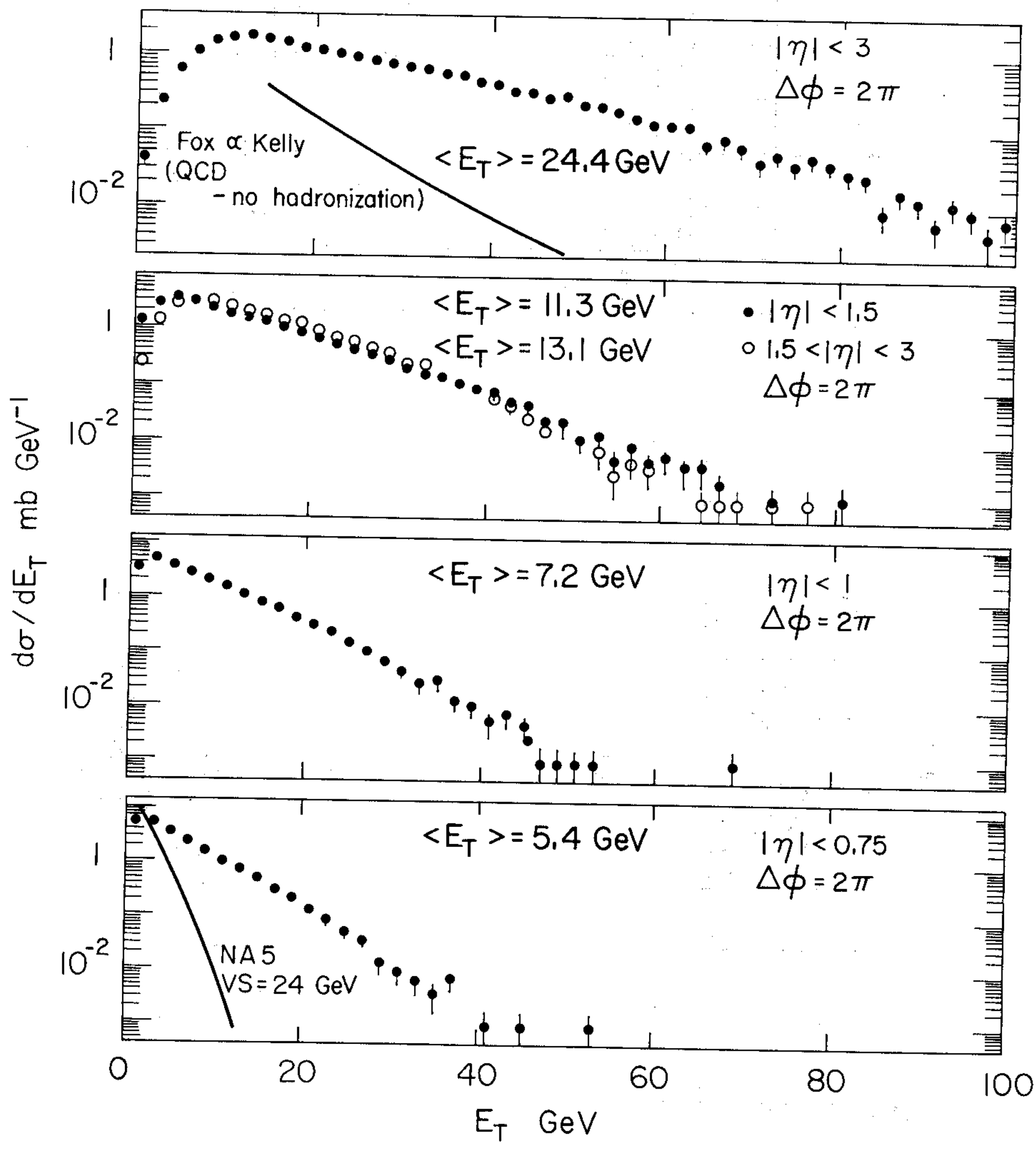
|η| < 3
Δφ = 2π
Fox α Kelly
(QCD
- no hadronization)
<ET> = 24.4 GeV
<ET> = 11.3 GeV
<ET> = 13.1 GeV
• |η| < 1.5
○ 1.5 < |η| < 3
Δφ = 2π
<ET> = 7.2 GeV
|η| < 1
Δφ = 2π
<ET> = 5.4 GeV
|η| < 0.75
Δφ = 2π
NA 5
VS = 24 GeV
dσ / dET mb GeV-1
1
10-2
0
20
40
60
80
100
ET GeV

Fig.2

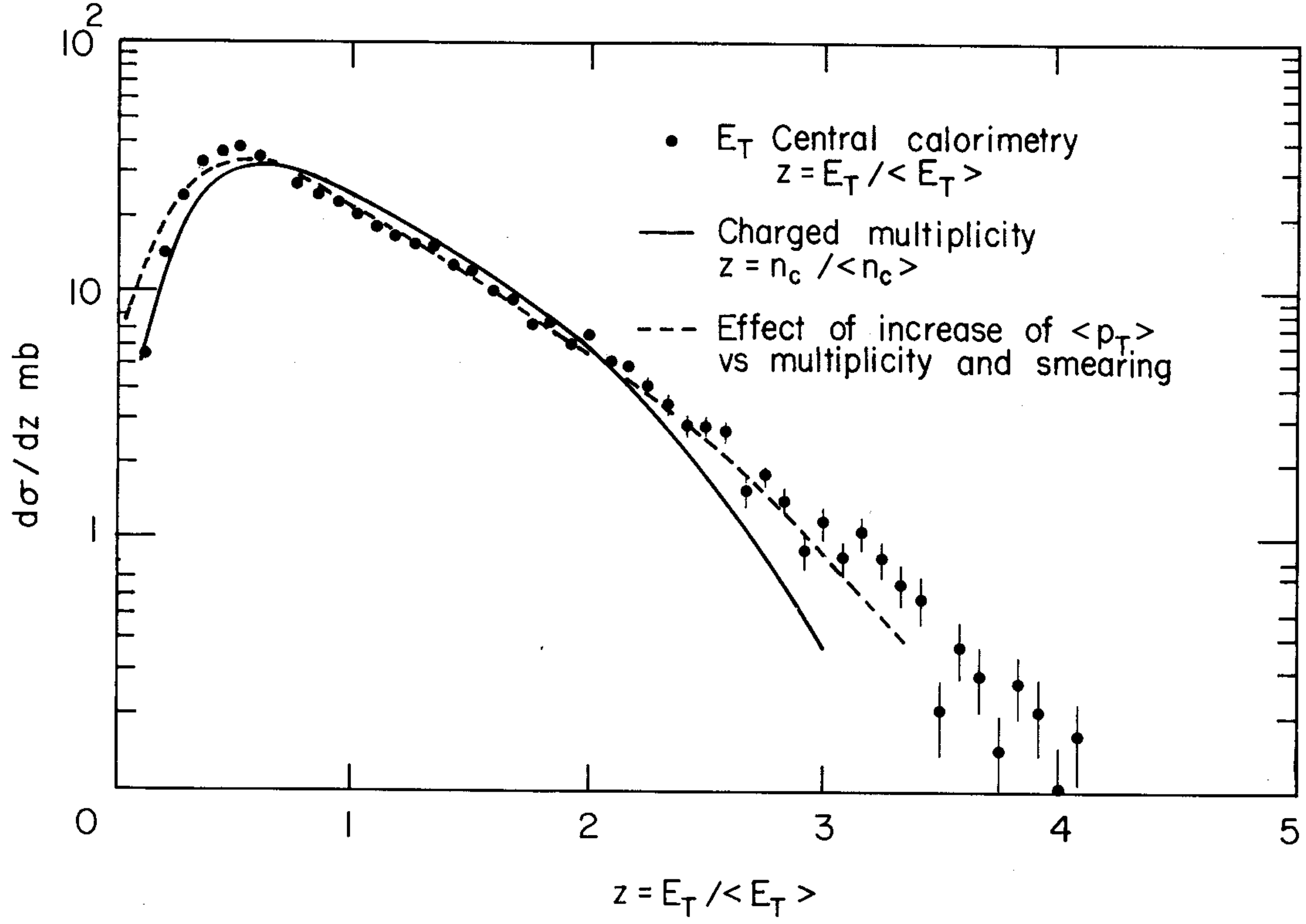

$10^2$
10
1
0
1
2
3
4
5
$d\sigma/dz$ mb
$z = E_T/\langle E_T \rangle$
• $E_T$ Central calorimetry $z = E_T/\langle E_T \rangle$
— Charged multiplicity $z = n_c/\langle n_c \rangle$
--- Effect of increase of $\langle p_T \rangle$ vs multiplicity and smearing


Fig.3

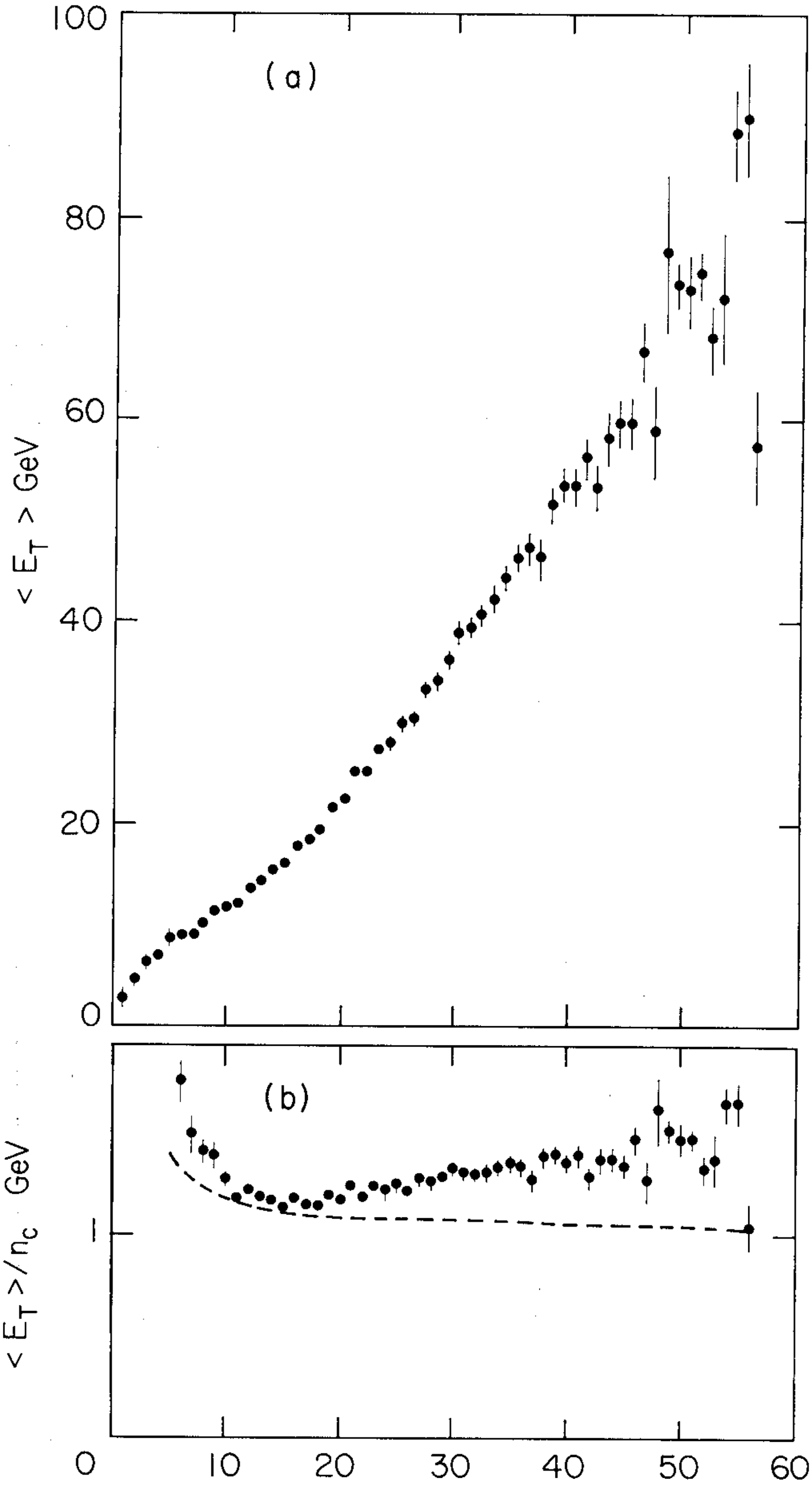


Fig.4